Available online at www.sciencedirect.com

ScienceDirect

Procedia Engineering 184 (2017) 399 – 408

Procedia Engineering

www.elsevier.com/locate/procedia

Advances in Material & Processing Technologies Conference

Surface Modification on CoCrMo Alloy to Improve the Adhesion Strength of Hydroxyapatite Coating

H. Mas Ayu[a,*], S. Izman[b], R. Daud[a], G. Krishnamurithy[c], A. Shah [d], S. H. Tomadi[a] and M. S. Salwani[a]

[a]*Faculty of Mechanical Engineering, Universiti Malaysia Pahang, 26600 Pekan, Pahang, Malaysia*
[b]*Faculty of Mechanical Engineering, Universiti Teknologi Malaysia, 81310 Skudai, Johor, Malaysia*
[c]*Department of Orthopaedic Surgery, NOCERAL, Faculty of Medicine, University of Malaya, 50603 Kuala Lumpur, Malaysia*
[d]*Universiti Pendidikan Sultan Idris, 35900 Tanjong Malim, Perak, Malaysia*

Abstract

Surface modification is often required in order to improve the biological and tribological properties of metallic implants. In the present study, Co-Cr-Mo alloy was oxidized in atmospheric condition to create oxide interlayer (Cr_2O_3) prior to hydroxyapatite (HA) coating. The effect of oxide interlayer on the adhesion strength of HA coating on oxidized Co-Cr-Mo substrate was investigated. The surface of oxide interlayer was rough and contained abundant of pores, which helps in providing better mechanical interlocking to HA coating. Scanning electron microscopy and X-ray diffraction techniques were used to characterize the surface morphology of the HA coating whilst a Revetest scratch test was used to measure the adhesion strength of HA coating on oxidized substrates. The oxide interlayer on the substrate was able to prevent severe cracks while maintaining the porosity of the coated layer. Scratch test results showed that adhesion strength of the HA coating on substrates with interlayer was significantly higher than those without interlayer (1.40 N Vs 1.04 N; $p<0.05$). Increasing sintering temperature increases adhesion strength proportionally. These findings suggest that the porous oxide interlayer provides better anchorage whilst minimizing surface cracks of HA on Co-Cr-Mo substrates.

Peer review under responsibility of the organizing committee of the Advances in Materials & Processing Technologies Conference

Keywords: Co-Cr-Mo alloy; Thermal oxidation; Hydroxyapatite; Dip coating; Adhesion strength

1. Introduction

Cobalt chromium molybdenum (Co-Cr-Mo) alloys have long being used for orthopaedic and dental implants due to their good mechanical and biocompatibility properties [1, 2]. To improve the implant performance, HA coatings

Peer review under responsibility of the organizing committee of the Advances in Materials & Processing Technologies Conference
doi:10.1016/j.proeng.2017.04.110

were introduced, resulting in increased implant bioactivity and bone bonding ability [3, 4]. It has also been demonstrated that HA reduces the release of potentially harmful metal ions and protects against corrosion [5-7]. Several methods of coating HA onto these implants have been previously described. These include plasma spraying [8], sputtering process [9, 10], biomimetic [11, 12], electrochemical deposition [13, 14] and sol-gel [13, 15, 16, 17]. Among these, the use of sol-gel technique provides many advantages: high HA purity, homogeneous composition and low synthesis temperature (25^{o}C - 800^{o}C) [4, 18, 19]. The use of direct sol-gel HA coating onto implants has been widely reported for titanium [15, 20-22] and steel based alloys [23-26]. However, the use of sol-gel technique on Co based implants have not been reported although the use of other techniques such as investment casting [27], electrophoretic deposition (EPD) [14] and biomimetic [28] have shown to been successful. Despite the many advantages of HA coating, poor adhesion strength between HA and the underlying substrate [29-31] and the low cohesive strength of the coated material [31, 32] are still major issues which remains unresolved. These issues often results in severe cracks and delamination of HA from the substrates, which would eventually lead to implant failure [29, 31-33]. To overcome these issues, researchers have designed an intermediate layer that, when placed between the brittle HA and the substrate, enhances the adhesive metal-ceramic (HA) bonding and coating integrity [24, 29]. As an example, the use of nitride as an interlayer on pure titanium prior to HA coating has been shown to improve adhesion ability dramatically [34]. However, many of the techniques and expertise required to produce this effect is costly and are usually technically challenging. Furthermore, the use of such techniques on Co-Cr-Mo alloys has never been established. In the present study, we describe a cheap, reliable and quick method to produce chromium oxide (Cr_2O_3) interlayer on Co-Cr-Mo substrate through an oxidation process prior to HA coating. To the best of our knowledge, this is the first study ever described using this technique for coating HA on Co-Cr-Mo alloy. The HA coating sintered at various temperatures on the Co-Cr-Mo substrate with and without the presence of oxide interlayer was then tested to prove that the method we developed produced improved adhesion strength.

2. Material and Methods

2.1. Substrate preparation

Co-Cr-Mo alloy (ASTM F-75) with carbon content of 0.24 wt % was used as the substrate. The rod substrate was cut using a precision cutter into small disk samples with a diameter and thickness of 14 mm and 2 mm respectively. Prior to the oxidation process, all samples preparation were ultrasonically cleaned with acetone for 30 minutes, followed by steam cleaning and finally were dried using a stream of compressed air as described earlier [35]. The initial surface finish of all samples were made constant at Ra = 0.1 ± 0.02 μm by grinding them using #500 SiC grit paper to ensure variation in surface roughness will not significantly influence the adhesion strength of oxide layer on the substrate.

2.2. Oxide interlayer generation and HA coating

The oxidation process was carried out at 1050°C for 3 hours in a muffle furnace under atmospheric condition and left to cool for 4 hours. The heating/cooling rate was set constant at approximately 5°C/min. This process creates the formation of oxide interlayer, which was confirmed using scanning electron microscope (SEM) analysis. Coating slurry was prepared by mixing 3 g of 75 μm grain sized HA powder into 10 ml of ethanol on a magnetic stirrer for 24 hours at room temperature (27°C). There were two groups of samples in this experiment i.e, the group with and without oxide interlayer. All samples were dip-coated with HA slurry was withdrawn from the slurry at a rate of 200 mm/min. The process (known as the dipping run) was repeated 4 times. Finally, HA coated substrates were sintered at three different temperatures 550°C, 650°C and 750°C for 1 hour at the heating/cooling rate of 1 °C/min.

2.3. Characterization techniques

Scanning electron microscope (SEM) was used to examine the surface morphology of the formed oxide interlayer and HA coating as well as their thickness on the substrates. X-ray diffraction (XRD) was used to characterize the phase composition of oxide layer and HA coating on the substrates.

2.4. Revetest scratch test

Revetest scratch test was used to determine the adhesion strength of oxide interlayer and HA coatings on the substrate. A sphere conical diamond having radius of 200 µm and angle of 120° was used as a stylus. Scratches on the oxidized substrate were conducted at a constant load rate of 30 N/min. Samples were displaced at a constant speed of 1.36 mm/min with maximum scratched coating length of 2 mm. A different set of scratching parameter was applied for measuring adhesion strength of HA coatings. The constant load rate applied was 1 N/min and the samples were moved at a constant speed of 1 mm/min with the same scratch length. The critical load of HA coating and oxide interlayer were measured 3 times on each sample at different position and was determined based on the friction coefficient obtained from the friction force graphs. SEM was used to image the scratches to confirm the failure distance.

2.5. Statistical analysis

The student t-test method was used as the mean comparative analysis tool. Each set of HA grain size and critical load results obtained from two sets of sintering temperatures were compared statistically against null hypothesis. SPSS ver. 17.0 statistical package software was used to evaluate the data obtained and the probability value (p-value) was set at <0.05 to be significant.

3. Results and Discussion

3.1. Oxidation phase characterization

Fig. 1(a) shows the morphology of Co-Cr-Mo substrate after undergone the oxidation process at 1050°C for 3 hours. The morphology of the particles appears blocky in shape with the size ranging from 100 nm to 700 nm. When compared to the images prior to oxidation, the increase in surface roughness was evident (0.1 µm vs. 1 µm). This may have been due to the increase in Cr_2O_3 grains size that is projecting towards the diffusion direction, thereby creating massive voids between them. The cross sectional view of the oxidized substrate demonstrates three distinct layers: the outer layer, inner layer and metal substrate (Fig. 1(b)). Although, the outer layer appears solid and more compact, it is approximately 5 times thinner than the inner layer. This suggests that internal oxidation may have occurred in this alloy just below the Cr rich oxide layer (outer layer). The inner layer shows the presence of porosity and micro-cracks indicating that their structure is less compact than the outer layer. Similar finding was also reported by Karalli et. al when oxidation process using tungsten on Co-Cr alloy was performed [36]. Blau et. al also reported same observation when they oxidized cobalt based alloys at lower temperature (850°C) with longer time durations [37]. Their results showed that the intergranular cracks were propagating below the compact Cr_2O_3 layer similar as seen in this study.

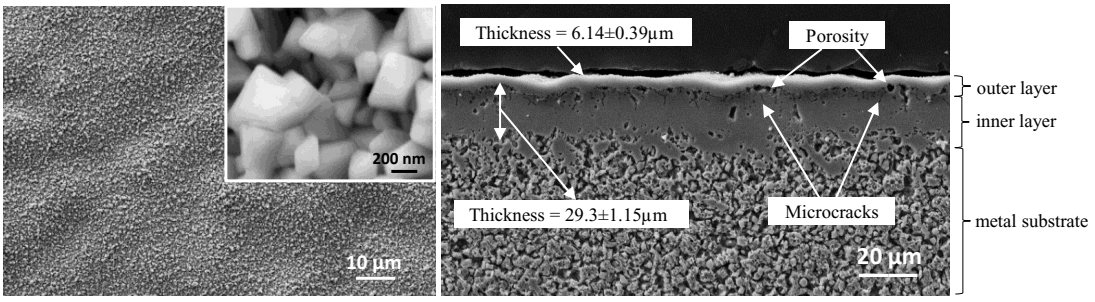

Fig. 1. (a) SEM micrographs of the oxidized HC Co-Cr-Mo sample prior to HA coating. (b) Cross-section image of oxidized HC Co-Cr-Mo 1050°C for 3 hours.

3.2. HA coating characterization

The surface morphologies of HA coatings on the substrate with and without oxidation were observed using SEM (Fig. 2 (a-d)). Although HA coatings were cracks in all substrates with or without oxide interlayer, a qualitative comparison showed that the substrate without oxide interlayer (Fig. 2d) had larger and severe cracks. This may have been attributed to the low cohesive strength between the HA coating itself and low adhesion strength between the coating and the substrate surface. It has been reported that HA coated on untreated and smooth substrate surface provides less gripping strength for the HA particles to anchor and therefore are easily cracks and delaminated from the substrate surface [38]. However, HA coating on oxidized substrates (Fig. 2b-c) has relatively lower and smaller cracks especially when sintering at higher temperatures (750°C). This is due to higher sintering temperature provided better chemical bonding and high densification of HA coating thus improved the adhesion strength [17]. HA grain size also is found to be increase when sintering temperature increase and appears to correlate with the reduction of cracks present on the coated substrate (Fig. 2c).

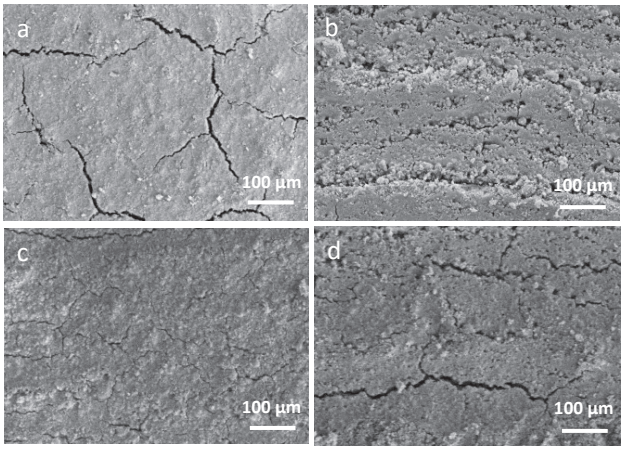

Fig. 2 The surface morphology of the HA coated samples after undergone various sintering temperature (a) 550°C with interlayer, (b) 650°C with interlayer, (c) 750°C with interlayer and (d) 750°C without interlayer.

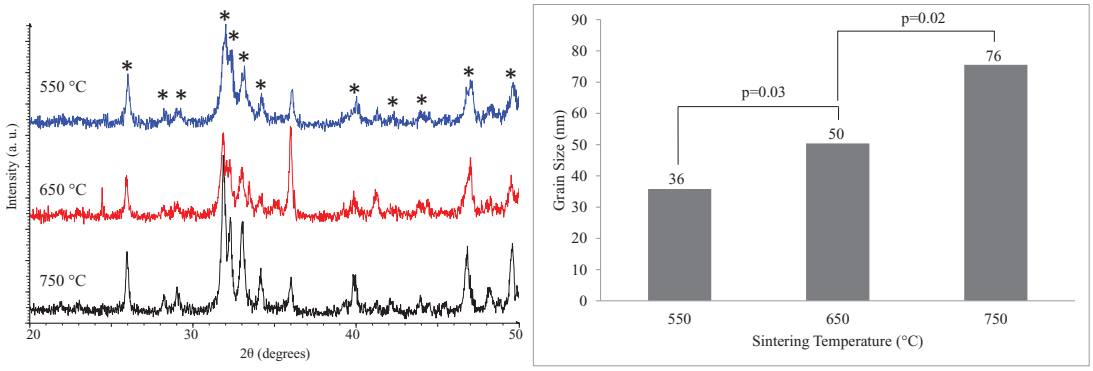

(a) (b)

Fig. 3 (a) XRD patterns for various sintering temperatures. The most intense HA ($Ca_5(PO_4)_3(OH)$) peaks are denoted by an asterisk *. (b) The variation of grain size as function of sintering temperature.

From the XRD patterns in Fig. 3(a), the calculated grain sizes revealed that the largest grain sizes (~76nm) is achieved when the composite is sintered at temperatures of 750°C, while the lowest (~36nm) is when it is sintered at 550°C. The results can be obtained in Fig. 3(b) and the difference in grain size is significant as $p<0.05$ according to statistical analysis software. The grain size values were calculated using the Debye-Sherrer formula [38] as shown in Eq. (3):

$$d = \frac{0.9\lambda}{\Delta_{2\theta}\cos\theta} \tag{3}$$

Where, d is the grain size, λ=0.1544 nm for wavelength of Cu Kα X-rays, and $\Delta_{2\theta}$ the full width at half maximum centered (FWHM) at angle 2θ (in radian). It is expected that grain size should be larger at higher sintering temperature than at lower sintering temperature. The degree of HA crystallization appears to increase with sintering temperature. The crystallization degree (X_C) of the samples was calculated from the following relation Eq. (4):

$$X_c \approx \frac{V_{112/300}}{I_{300}} \tag{4}$$

Where, $V_{112/300}$ is the intensity of the hollow between (112) and (300) reflections, and I_{300} is the intensity of the reflection belonging to (300) plane [39]. The degree of the crystallization increased with the increase in the sintering temperature from 0.57, 0.6 and 0.75 at temperature 550°C, 650°C and 750°C respectively.

These finding appears to support previous results [38, 40-42]. No other crystalline phase such as calcium carbonate or calcium oxide was present at temperature ranging from 550°C to 750°C. It has also been reported that HA decomposed into other phase such as α- and β-tetracalcium phosphate at the temperature of 800°C and above due to dehydroxylation and fully crystalline occurs at temperature above 500°C [43], due to this reason the sintering temperature was selected below this temperature.

As can be seen from Figure 3(a), Cr_2O_3 phase diffraction peaks at temperature 650°C is narrower and had higher intensity compared to diffraction peaks at temperature 550°C. This evidence indicates that the grain size of polycrystalline chromium oxide (Cr_2O_3) increased with sintering temperature [40]. However, it is important to report that XRD patterns of substrate sintered at temperature 750°C shows weaker diffraction peaks of Cr_2O_3 compared to substrate sintered at 650°C. This phenomenon probably due to compact HA layer with larger grain size of HA have become as diffusion barrier to prevent oxygen from continuously react with chromium element. This result is in correlation with a report by Chen et. al who found that the oriented crystalline ZrN films with larger grain sizes provide a higher activation energy against Cu diffusion and can act as an excellent diffusion barrier for Cu up to 800°C on silicon substrate [44].

Additionally, the cross section of the HA coatings on unoxidized and oxidized Co-Cr-Mo substrates also were examined using the SEM, as shown in Fig. 4. According to the different atomic contrast of HA coatings and Co-Cr-Mo substrate, the bright regions in Fig. 4 were determined as metal substrate, as well as the top outer regions which is dark regions is HA coatings. It is noted that with the increment of sintering temperature, the thickness of HA layers are decreasing rapidly while the thickness of oxide layers are increasing respectively. The thickness of HA layer after sintering at temperature ranging from 550°C to 750°C showed decrement from 50.18 ± 0.7 μm to 12.73 ± 0.75 μm respectively. Although Cr_2O_3 formation at the interface between the HA layer and substrate might help to anchor the HA grain particles [15], but thicker HA layer at this stage might weaken this effect so that a lower adhesive strength is obtained. Similar results are observed in HA coating without oxide interlayer on the Co-Cr-Mo substrate as shown in Fig. 4(d). Even though in the cross-section images (Fig. 4 (a-c)), cracks and pores still presence in the HA coatings on oxidized substrate, but the chemical bonding of HA with the oxide interlayer showed better than without it. From Fig. 4(a), the cross-section SEM image revealed no cracks at the interface of HA coating and the oxide interlayer. This means that oxide interlayer have improved the adhesive strength of HA on the substrate surface. While, in Fig. 4(d) cross-section image clearly showed severe long cracks are distributed across the HA coating with weaker bonding strength between HA and the unoxidized substrate. Fig. 4(b) displays several small cracks were observed in the HA coating on oxidized substrate at sintering temperature of 650°C.

However, at this temperature the chemical bonding of HA with the interlayer is only partially crystallized. It is concluded that at sintering temperature 650°C might not be able to convert the coating to high quality of HA layer therefore higher sintering temperature is required. The cross-section image shown in Fig. 4(c) looks denser HA coating with porous surface after sintering at temperature 750°C. This is due to at high temperature the density of HA increased thus stronger agglomerates of HA occurred and become more compact with thinner HA thickness [45]. The formation of porous structure is useful to tailor HA coatings to the substrate thus, enhances the adhesion strength of the HA coatings [39].

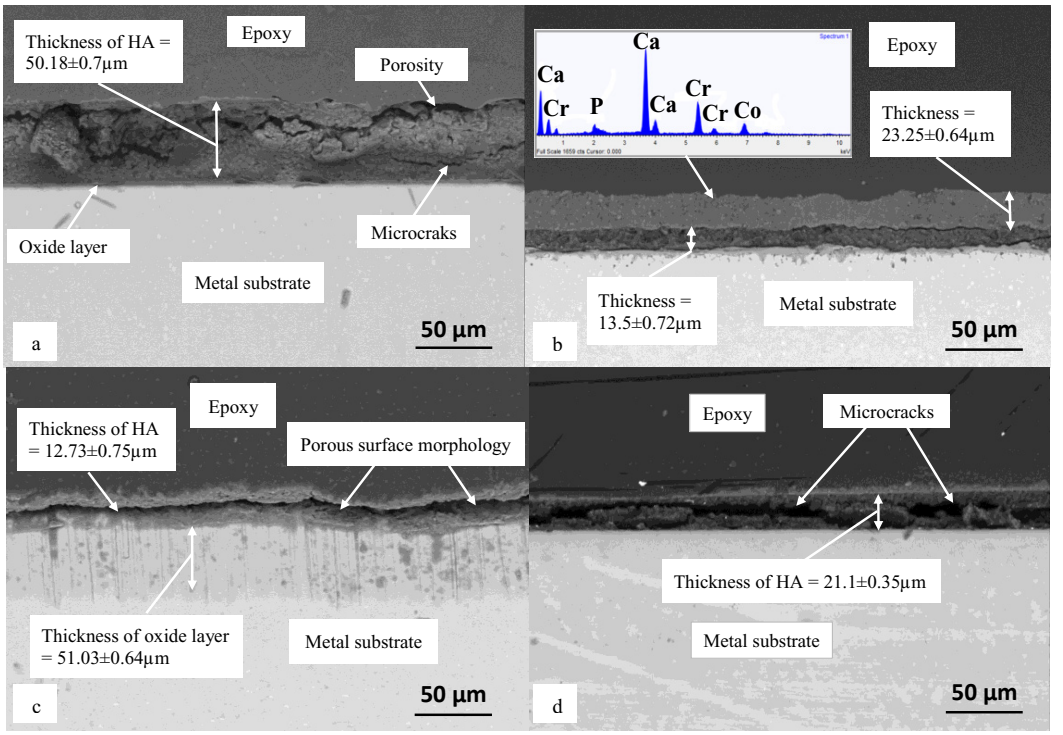

Fig. 4 Cross-section image of HA coated substrate with interlayer sintered at various temperature, (a) 550°C with interlayer, (b) 650°C with interlayer, (c) 750°C with interlayer and (d) 750°C without interlayer.

3.3. Adhesion strength of HA coatings

Adhesion strength of HA coating was examined by Revertest scratch tester. The test measures the critical load required to remove the coating from the substrate at a constant speed with progressive load. The progressive load applied in this experiment was found sufficient to completely delaminate all HA coating layers deposited on Co-Cr-Mo substrates. Graphs were plotted which record the changes in friction coefficient, friction force and normal loads during the scratch tests are represented in Fig. 5 (a-e). Normal load graphs increase linearly in all conditions which represent constant load increment of 1 N/min during scratching. This plot always appears in above friction coefficient (red colour) and friction forces (purple colour) graphs. The coating fails at the critical load range from 1.04 to 1.34 N with sintering temperature from 550°C to 750°C respectively. The critical load of coating failure was determined by the software (Scratch test software, Version 4.33, Switzerland).

The adhesion strength between the coating and substrate comes from two aspects, the mechanical interlocking and the chemical bonding. In current work, since the substrates had the same surface finish, the mechanical interlocking can be considered identical. Therefore, the increase in the adhesion strength is attributed to the stronger chemical bonds, which were developed at the coating-substrate interface during coating deposition process,

especially at the sintering stage. From the scratch test results obtained in this study, the incorporation of oxide interlayer with the increment of sintering temperature accompanies increased of scratch adhesion as illustrated in Fig 6. The difference in scratch results for all sintering temperature is significant as $p<0.05$.

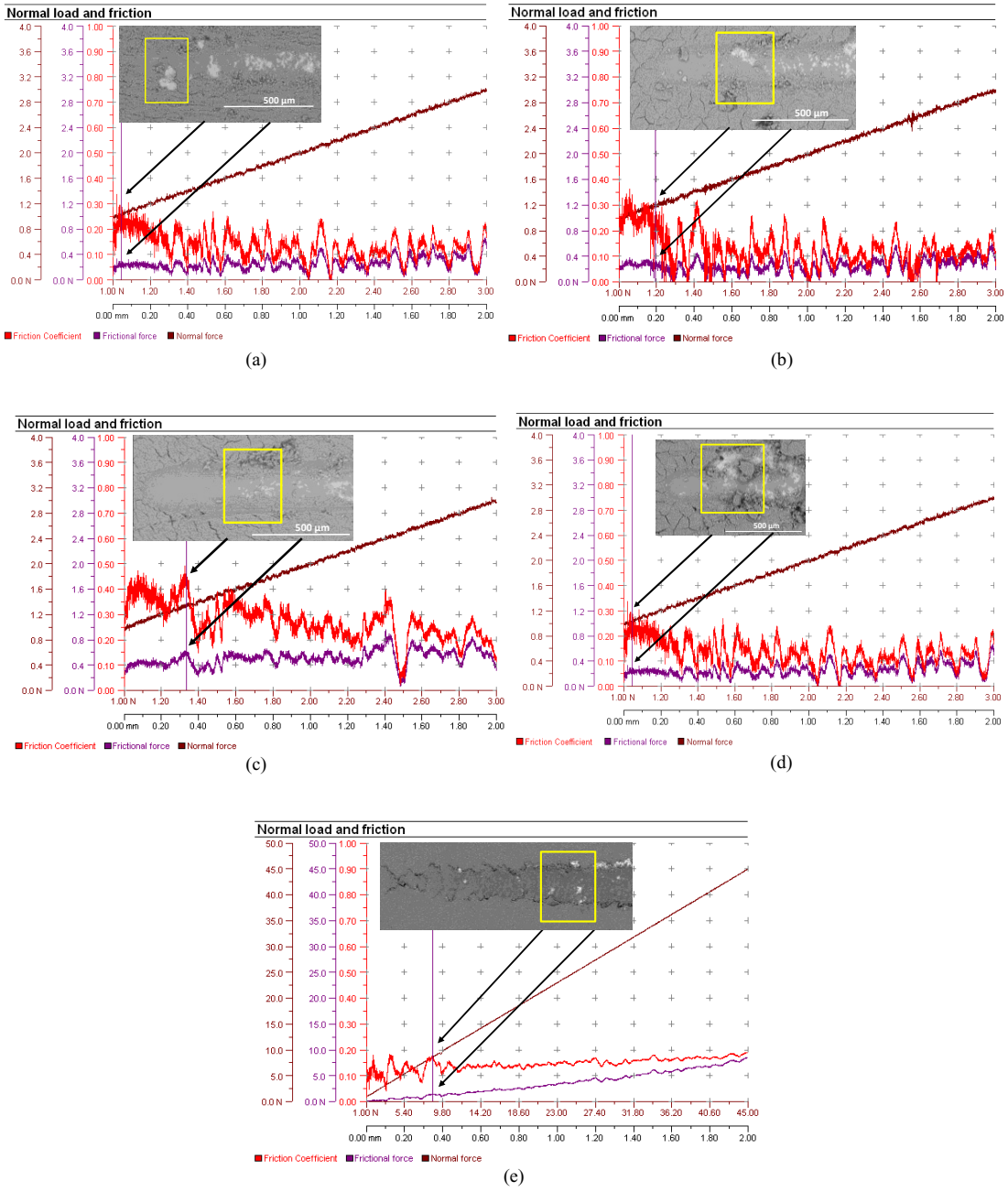

Fig. 5 SEM image of scratch tracks along with graphs of friction coefficient, friction force and normal forces at various sintering temperature with and without interlayer, (a) 550°C with interlayer, (b) 650°C with interlayer, (c) 750°C with interlayer and (d) 750°C without interlayer, (e) Oxide interlayer at temperature 1050°C.

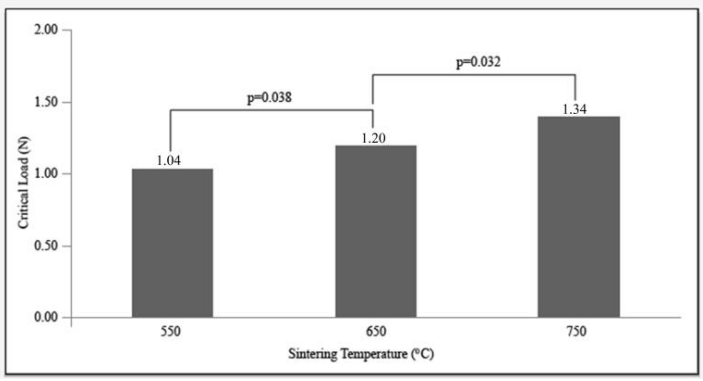

Fig. 6 The variation of critical load as function of sintering temperature.

4. Conclusion

The adhesion strength of HA coatings with and without oxide interlayer are characterized using SEM, XRD and scratch test. It was found that:

1. The HA coatings prepared through sol-gel dip coating method demonstrate severe cracks surface morphology under various tested sintering temperature. However, at sintering temperature 750°C, the cracks surface were less and smaller compared to low sintering temperatures (550°C and 650°C). These results showed better adhesion strength of HA to Co-Cr-Mo substrate at higher temperature (above 700°C).
2. Critical load, Lc was increased from 1.04 N to 1.34 N as well as grain sizes from 36 nm to 76 nm, when the sintering temperature increases up to 750ºC. The difference in Lc and grain sizes obtained in this study is significantly as $p \leqslant 0.05$ according to statistical analysis software.
3. The incorporation of oxide interlayer prior to HA coating proven to promote better anchorage for HA particles and minimized the cracks surface compared to HA coated on Co-Cr-Mo substrate without oxide interlayer.
4. High Lc (8.63N) obtained for oxide interlayer proven that oxide layer have good adhesion to the substrate thus, promote better anchor for HA to adhere and more stable HA coating over time.
5. The higher the sintering temperature will increase the fracture toughness of the HA coatings thus, increased the adhesion strength between HA coating and metal substrate. While, at lower sintering temperature (below 700°C) cracks surface were observed as means of low fracture toughness of the coatings.
6. As the sintering temperature increased from 550°C to 750°C, it is found that the thickness of HA layers were decreased while the thickness of oxide layer increased rapidly.

Further investigation on in-vitro test will be done to confirm that cells proliferation and toxicity level on HA coated with the presence of oxide interlayer in Co-Cr-Mo substrates.

Acknowledgement

This research is fully supported by research grant RDU1403118 provided by Faculty of Mechanical Engineering, Universiti Malaysia Pahang (UMP). The authors also fully acknowledged Faculty of Mechanical Engineering, Universiti Teknologi Malaysia (UTM) and Universiti Tun Hussein Onn Malaysia (UTHM) for providing their facilities in conducting this research respectively.

References

[1] A. Igual Muñoz and S. Mischler, Effect of the Environment on Wear Ranking and Corrosion of Biomedical Cocrmo Alloys, J. Mater. Sci.: Mater. Med. 22 (2011) 437-450.

[2] S. Izman, Mohammed Rafiq Abdul-Kadir, Mahmood Anwar, E. M. Nazim, R. Rosliza, A. Shah and M. A. Hassan. Surface Modification Techniques for Biomedical Grade of Titanium Alloys: Oxidation, Carburization and Ion Implantation Processes. 2012, ISBN: 978-953-51-0354-7.

[3] C. Ergun, R. H. Doremus and W. A. Lanford, Interface Reaction/Diffusion in Hydroxylapatite-Coated SS316L and CoCrMo Alloys, Acta Mater. 52 (2004) 4767-4772.

[4] M.-F. Hsieh, L.-H. Perng, T.-S. Chin and H.-G. Perng, Phase Purity of Sol–Gel-Derived Hydroxyapatite Ceramic, Biomaterials. 22 (2001) 2601-2607.

[5] T. Wang and A. Dorner-Reisel, Effect of Substrate Oxidation on Improving the Quality of Hydroxyapatite Coating on CoNiCrMo, J. Mater. Sci. 39 (2004) 4309-4312.

[6] S. Zhang, Y. S. Wang, X. T. Zeng, K. A. Khor, W. Weng and S. E. Sun, Evaluation of Adhesion Strength and Toughness of Fluoridated Hydroxyapatite Coatings, Thin Solid Films. 516 (2008) 5162-5167.

[7] M. Cavalli, G. Gnappi, A. Montenero, D. Bersani, P. P. Lottici, S. Kaciulis, G. Mattogno and M. Fini, Hydroxy- and Fluorapatite Films on Ti Alloy Substrates: Sol-Gel Preparation and Characterization, J. Mater. Sci. 36 (2001) 3253-3260.

[8] C. Y. Yang, B. C. Wang, W. J. Chang, E. Chang and J. D. Wu, Mechanical and Histological Evaluations of Cobalt-Chromium Alloy and Hydroxyapatite Plasma-Sprayed Coatings in Bone, J. Mater. Sc.: Mater. Med. 7 (1996) 167-174.

[9] Y. Yunzhi, K. Kyo Han and L. O. Joo, A Review on Calcium Phosphate Coatings Produced Using a Sputtering Process-an Alternative to Plasma Spraying, Biomaterials. 26 (2005) 327-337.

[10] S.-J. Ding, C.-P. Ju and J.-H. C. Lin, Characterization of Hydroxyapatite and Titanium Coatings Sputtered on Ti-6al-4v Substrate, J. Biomed. Mater. Res. 44 (1999) 266-279.

[11] J. C. Escobedo Bocardo, M. A. López Heredia, D. A. Cortés Hernández, A. Medina Ramírez and J. M. Almanza Robles, Apatite Formation on Cobalt and Titanium Alloys by a Biomimetic Process, Adv. Technol. Mater. & Mater. Process. 7 (2005) 141-148.

[12] D. A. Cortés-Hernández, J. C. Escobedo-Bocardo, A. A. Nogiwa-Valdez and R. Muñoz, Biomimetic Bonelike Apatite Coating on Cobalt Based Alloys, Mater. Sci. Forum. 442 (2003) 61-66.

[13] R. I. M. Asri, W. S. W. Harun, M. A. Hassan, S. A. C. Ghani and Z. Buyong. A Review of Hydroxyapatite-Based Coating Techniques: Sol-Gel and Electrochemical Depositions on Biocompatible Metals. Journal of the Mechanical behaviour of Biomedical Materials. 57 (2016) 95-108.

[14] W. Lu Ning and L. Jing Li, Preparation of Hydroxyapatite Coating on Co-Cr-Mo Implant Using an Effective Electrochemically-Assisted Deposition Pretreatment, Mater. Charac. 62 (2011) 1076-1086.

[15] H. Mas-Ayu, S. Izman, Mohammed Rafiq Abdul-Kadir, Rosdi Daud, A. Shah, Mohd Faiz Mohd Yusoff, M. W. Shamsiah, T. M. Yong and T. Kamarul. Influence of Carbon Concentrations in Reducing CO and cr Ions Release in Cobalt Based Implant: A Preliminary Report. Advanced Materials Research. 845 (2014) 462-466.

[16] W. Diangang, C. Chuanzhong, H. Ting and L. Tingquan, Hydroxyapatite Coating on Ti6al4v Alloy by a Sol–Gel Method, J. Mater. Sci.: Mater. Med. 19 (2008) 2281-2286.

[17] M. Y. Mohd Faiz, A. K. Mohammed Rafiq, I. Nida, H. Mas Ayu and H. Rafaqat. Dipcoating of Poly (Ɛ-Caprolactone)/Hydroxyapatite Composite Coating on Ti6Al4V for Enhanced Corrosion Protection, Surf. Coat. Technol. 245 (2014) 102-107.

[18] C. J. Brinker, G. C. Frye, A. J. Hurd and C. S. Ashley, Fundamentals of Sol-Gel Dip Coating, Thin Solid Films. 201 (1991) 97-108.

[19] P. Shi, W. F. Ng, M. H. Wong and F. T. Cheng, Improvement of Corrosion Resistance of Pure Magnesium in Hanks' Solution by Microarc Oxidation with Sol–Gel TiO_2 Sealing, J. Alloys & Comp. 469 (2009) 286-292.

[20] H.-W. Kim, H.-E. Kim and J. C. Knowles, Fluor-Hydroxyapatite Sol–Gel Coating on Titanium Substrate for Hard Tissue Implants, Biomaterials. 25 (2004) 3351-3358.

[21] S. Zhang, Z. Xianting, W. Yongsheng, C. Kui and W. Wenjian, Adhesion Strength of Sol–Gel Derived Fluoridated Hydroxyapatite Coatings, Surf. Coat. Technol. 200 (2006) 6350-6354.

[22] Y. Wang, S. Zhang, X. Zeng, L. L. Ma, W. Weng, W. Yan and M. Qian, Osteoblastic Cell Response on Fluoridated Hydroxyapatite Coatings, Acta Biomater. 3 (2007) 191-197.

[23] D.-M. Liu, Q. Yang and T. Troczynski, Sol–Gel Hydroxyapatite Coatings on Stainless Steel Substrates, Biomaterials. 23 (2002) 691-698.

[24] C. García, S. Ceré and A. Durán, Bioactive Coatings Prepared by Sol–Gel on Stainless Steel 316L, J. Non-Cryst. Solids. 348 (2004) 218-224.

[25] U. Vijayalakshmi, K. Prabakaran and S. Rajeswari, Preparation and Characterization of Sol–Gel Hydroxyapatite and Its Electrochemical Evaluation for Biomedical Applications, J. Biomed. Mater. Res.: Part A. 87A (2008) 739-749.

[26] A. Dey, A. K. Mukhopadhyay, S. Gangadharan, M. K. Sinha, D. Basu and N. R. Bandyopadhyay, Nanoindentation Study of Microplasma Sprayed Hydroxyapatite Coating, Ceram. Int. 35 (2009) 2295-2304.

[27] H. Minouei, M. Meratian, M. Fathi and H. Ghazvinizadeh, Biphasic Calcium Phosphate Coating on Cobalt-Base Surgical Alloy During Investment Casting, J. Mater. Sci.: Mater. Med. 22 (2011) 2449-2455.

[28] D. Ke, T. Allen and W. Rizhi, A New Evaporation-Based Method for the Preparation of Biomimetic Calcium Phosphate Coatings on Metals, Mater. Sci. Eng.: Part C. 29 (2009) 1334-1337.

[29] Y. C. Yang and B. Y. Chou, Bonding Strength Investigation of Plasma-Sprayed HA Coatings on Alumina Substrate with Porcelain Intermediate Layer, Mater. Chem. Phys. 104 (2007) 312-319.

[30] E. D. Case, I. O. Smith and M. J. Baumann, Microcracking and Porosity in Calcium Phosphates and the Implications for Bone Tissue Engineering, Mater. Sc. Eng.: Part A. 390 (2005) 246-254.
[31] W. Zhen-lin and Z. Rong-chang, Comparison in Characterization of Composite and Sol-Gel Coating on AZ31 Magnesium Alloy, Trans. Nonferrous Metals Soc. China. 20 (2010) 665-669.
[32] R. Roest, B. A. Latella, G. Heness and B. Ben-Nissan, Adhesion of Sol–Gel Derived Hydroxyapatite Nanocoatings on Anodised Pure Titanium and Titanium (Ti6Al4V) Alloy Substrates, Surf. Coat. Technol. 205 (2011) 3520-3529.
[33] P. B. Kirk and R. M. Pilliar, The Deformation Response of Sol-Gel Derived Zirconia Thin Films on 316l Stainless Steel Substrates Using a Substrate Straining Test, J. Mater. Sci. 34 (1999) 3967-3975.
[34] H. C. Man, K. Y. Chiu, F. T. Cheng and K. H. Wong, Adhesion Study of Pulsed Laser Deposited Hydroxyapatite Coating on Laser Surface Nitrided Titanium, Thin Solid Films. 517 (2009) 5496-5501.
[35] S. Izman, M. A. Hassan, A. K. Mohammed Rafiq, M. R. Abdullah, M. Anwar, A. Shah and R. Daud, Effect of Pretreatment Process on Thermal Oxidation of Biomedical Grade Cobalt Based Alloy, Adv. Mat. Res. 399-401 (2011) 1564-1567.
[36] A. Karaali, K. Mirouh, S. Hamamda and P. Guiraldenq, Effect of Tungsten 0-8 wt.% on the Oxidation of Co-Cr Alloys, Comp. Mater. Sci. 33 (2005) 37-43.
[37] P. J. Blau, T. M. Brummett and B. A. Pint, Effects of Prior Surface Damage on High-Temperature Oxidation of Fe-, Ni-, and Co-Based Alloys, Wear. 267 (2009) 380-386.
[38] S. Mudenda, K. L. Streib, D. Adams, J. W. Mayer, R. Nemutudi and T. L. Alford, Effect of Substrate Patterning on Hydroxyapatite Sol–Gel Thin Film Growth, Thin Solid Films. 519 (2011) 5603-5608.
[39] O. Kaygili, C. Tatar and F. Yakuphanoglu, Structural and Dielectrical Properties of Mg_3–$Ca_3(PO_4)_2$ Bioceramics Obtained from Hydroxyapatite by Sol–Gel Method, Ceramics International. 38 (2012) 5713-5722.
[40] X. Pang, K. Gao, F. Luo, H. Yang, L. Qiao, Y. Wang and A. A. Volinsky, Annealing Effects on Microstructure and Mechanical Properties of Chromium Oxide Coatings, Thin Solid Films. 516 (2008) 4685-4689.
[41] I.-S. Kim and P. N. Kumta, Sol–Gel Synthesis and Characterization of Nanostructured Hydroxyapatite Powder, Mat. Sc. Eng. B. 111 (2004) 232-236.
[42] M. H. Fathi and A. Hanifi, Evaluation and Characterization of Nanostructure Hydroxyapatite Powder Prepared by Simple Sol–Gel Method, Mater. Lett. 61 (2007) 3978-3983.
[43] C. M. Lopatin, V. B. Pizziconi and T. L. Alford, Crystallization Kinetics of Sol-Gel Derived Hydroxyapatite Thin Films, J. Mater. Sc.: Mater. Med. 12 (2001) 767-773.
[44] C. S. Chen, C. P. Liu, H. G. Yang and C. Y. A. Tsao, Influence of the Preferred Orientation and Thickness of Zirconium Nitride Films on the Diffusion Property in Copper, J. Vac. Sc. Tech. B. 22 (2004) 1075-1083.
[45] D. Veljovic, R. Jancic-Hajneman, I. Balac, B. Jokic, S. Putic, R. Petrovic and D. Janackovic, The Effect of the Shape and Size of the Pores on the Mechanical Properties of Porous HaP-Based Bioceramics, Ceram. Int. 37 (2011) 471-479.